Multifocusing as a method of improving subsurface imaging

Alex Berkovitch and Igor Belfer, Geomage, Modiin, Israel
Evgeny Landa, OPERA, Pau, France

Imaging the subsurface, the ultimate goal of the seismic method, can be done in different ways and in different domains: time or depth. Although depth migration has become almost mandatory in areas of complex geology—because it accounts for traveltime nonhyperbolic moveout, it has, in fact, quite a limited purpose—to convert seismic data from one form to another for a *given velocity model*. Time imaging provides sufficient information for a subsurface of moderate complexity. Moreover, even for complex areas that require depth migration for correct subsurface imaging, time imaging usually constitutes a key first step that facilitates the estimation of a velocity model for depth imaging. For these reasons, improving the quality of time imaging is a focus of intensive research. A recent advance is multifocusing (MF), a method with the potential to greatly improve the quality of time imaging.

Many research efforts have sought to improve the accuracy of moveout corrections. In particular, different traveltime equations have been proposed whose goal was improving the quality of CMP (common midpoint) stacks through better alignment of reflection events within a single CMP gather. It has long been recognized that, for a horizontally layered and isotropic overburden, the standard Dix NMO (normal movement) equation

$$t = \sqrt{t_0^2 + x^2 / V_{RMS}^2} \qquad (1)$$

is a second-order approximation (in offset) of the full traveltime expansion that can be represented by an infinite even-powered Taylor series. In Equation 1, t is the traveltime from the source to the reflector and back to the receiver, t_0 is the vertical traveltime from the surface to the reflector, x is the distance from the shot to the receiver (offset), and V_{RMS} is the rms velocity.

The use of higher-order approximations of such series for NMO corrections also is possible; such approximations have proved useful for analysis of individual CMP records. However, higher-order approximations are of little use in stacking procedures mainly because, with a multiparameter search based on the same amount of data (CMP gather), the stacking procedure becomes less robust.

De Bazelaire (1988) proposed an alternative approach to NMO correction, using the so-called shifted hyperbola equation

$$t = t_0 - t_p + \sqrt{t_p^2 + x^2 / V^2} \qquad (2)$$

For a given t_0, Equation 2 is an expansion of the traveltime with two independent parameters: t_P and V. The traveltime approximation given by Equation 2, when represented as a series in t^2, is exact through fourth order in offset while still retaining the hyperbolic character of the traveltime. For sufficiently small offsets, the parameter V may be replaced by a constant near-surface velocity V_o, resulting in a robust single-parameter correlation/stacking procedure.

In contrast to the procedures discussed above, the MF approach proposed by Berkovitch et. al. (1994) is based on homeomorphic imaging theory (Gelchinsky et. al., 1992.) In MF, each zero-offset trace is constructed by stacking traces that need not belong to the same CMP gather but, rather, whose
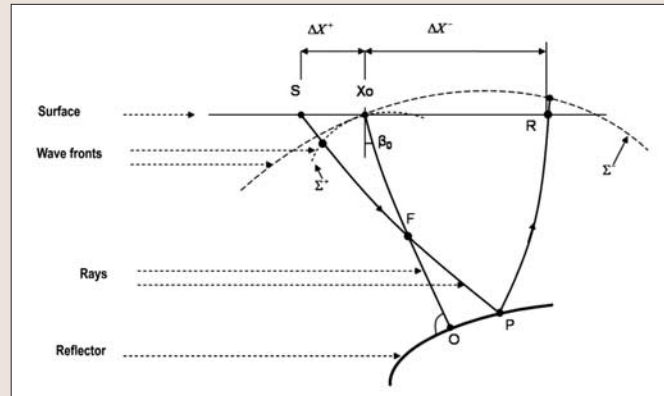

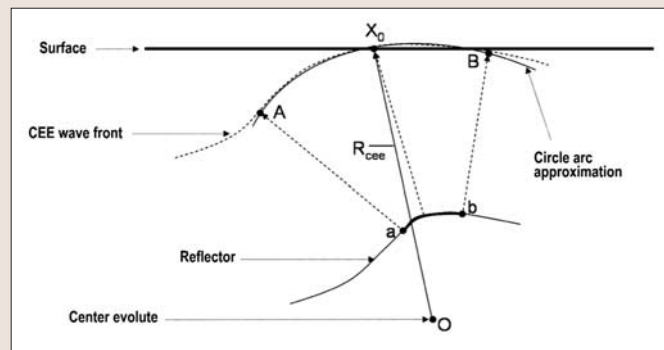*Figure 1. A schematic representation of the focusing principle.*

Figure 2. A schematic representation of CEE wavefront formation.

sources and receivers are within the limits of a certain superbase in the vicinity of the central point. The size of such a superbase is determined by the size of the Fresnel zone. The number of traces falling in this zone can significantly exceed the number of traces belonging to one CMP gather. This allows a considerable increase in the signal-to-noise ratio for the target reflection. Since the traces being stacked no longer belong to the same CMP gather, this procedure requires a more general moveout correction than the one used in conventional CMP stacking. For a given source-receiver pair, the multifocusing moveout equation is based on spherical approximation of reflection event's wavefront near the observation surface.

In a 2D case, this new time correction depends on three parameters measured at the central point. In other words, the moveout correction expressed by the multifocusing formula is a three-parameter expansion of the traveltime in the vicinity of the central point. Hence, it is closely related to paraxial ray approximation. The three parameters are: the emergence angle β and the radii of curvature R_{cre} and R_{cee} of the two fundamental wavefronts that will be described later.

An alternative approach for zero-offset time imaging for arbitrary source-receiver positions is the so-called common reflection surface (CRS) stacking method, proposed by Müller et al. (1998). Staking parameters proposed in this method, namely, the radius of curvature of the normal incident point wave (R_{NIP}) and the radius of curvature of the normal wave (R_N) are essentially the same parameters as R_{cre} and R_{cee} as in the MF method.

MF traveltime formulas provide an adequate representation of arrival times for arbitrary source-receiver configurations, just like the conventional NMO correction does for CMP gathers. For a single CMP gather, the MF moveout correction reduces to de Bazelaire's shifted hyperbola. It is well known that Equation 2 approximates traveltimes for a horizontally layered medium superior to that of the classical Dix NMO equation. The MF correction formula is remarkably accurate even for strong curved reflectors. This can be attributed to the fact that it is not a simple hyperbolic Taylor expansion but a double square root.

It should be emphasized that the multifocusing moveout correction is an appropriate basis for a stacking procedure, as it can align reflection events in a large gather of seismic traces (superbase) that spans many CMP gathers. Implementation of the multifocusing method is technically challenging because it requires defining three moveout parameters instead of a single parameter (stacking velocity) in standard NMO velocity analysis. Although, in principle "mixing" reflection events from a number of CMP gathers (in other words a number of depth reflection points) may compromise special resolution of the resulting stacked section and make random noise appear as an interpretable signal, our implementation of a simultaneous three-parameter search mostly avoids this effect and minimizes artifacts.

The aim of this paper is to demonstrate practical feasibility of MF method, and to compare multifocusing time sections with conventional NMO/DMO stacked sections.

MF moveout correction. Let us consider the ray diagram in Figure 1. A normal ray starts at the surface point X_0 (which is referred to as the central point) with the angle β to the vertical hits the reflector at the normal incident point O and returns back to X_0. A paraxial ray from arbitrary source S crosses the central ray at point F and arrives at receiver R. F can be considered as a fictitious source of two fictitious waves with the wavefront rays Σ^+ (emitting from F upward to the surface) and Σ^- (emitting from the point F downward, reflected at the reflector and emerging again at the point X_0). The moveout correction for an arbitrary source-receiver configuration in the vicinity of the normal ray in this case can be written (Berkovitch et al., 1994):

$$\Delta\tau = \frac{\sqrt{\left(R^+\right)^2 + 2R^+\Delta X^+ \sin\beta + \left(\Delta X^+\right)^2} - R^+}{V_0} + \frac{\sqrt{\left(R^-\right)^2 + 2R^-\Delta X^- \sin\beta + \left(\Delta X^-\right)^2} - R^-}{V_0}$$ (3)

where

$$R^+ = \frac{1+\sigma}{\dfrac{1}{R_{cee}} + \dfrac{\sigma}{R_{cre}}},$$ (4)

$$R^- = \frac{1-\sigma}{\dfrac{1}{R_{cee}} - \dfrac{\sigma}{R_{cre}}},$$ (5)

and σ is the so-called focusing parameter given by

$$\sigma = \frac{\Delta X^+ - \Delta X^-}{\Delta X^+ + \Delta X^- + 2\dfrac{\Delta X^+ \Delta X^-}{R_{cre}}\sin\beta}.$$ (6)
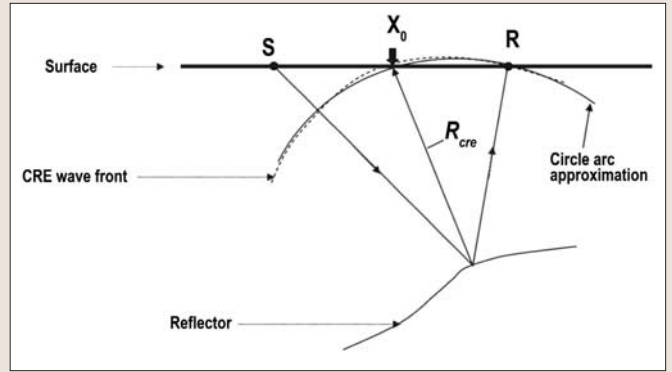

Figure 3. A schematic representation of CRE wavefront formation.

In the above equations, ΔX^+ and ΔX^- are the distances between source and receiver, respectively, for a given trace with respect to the central ray, R^+ and R^- are the radii of curvature of the fictitious wavefronts Σ^+ and Σ^- in the vertical plane respectively, and V_0 is the near-surface velocity which is assumed constant along the horizontal observation line. Finally, R_{cee} and R_{cre} denote the radii of curvature of the two fundamental wavefronts.

The first front is the CEE wavefront, which is formed by normal rays emitted by different points on the reflector (like in an "exploding reflector" scenario, shown in Figure 2). The second front is the CRE wavefront, which is formed by a source where the zero-offset ray emitted from the central point hits the reflector (Figure 3).

Equation 3 can be understood using the concept of an *auxiliary medium* when the real medium is replaced by a homogeneous one with the velocity equal to the near-surface velocity V_0. In the auxiliary medium, both the central and paraxial rays will be represented by combinations of straight line segments. Consider again the ray diagram in Figure 1.

For a source at point S and receiver at point R, the first term on the right side of Equation 3 corresponds to the time along the ray segment SF that can be obtained from triangle SFX_0. The second term corresponds to the time along the ray FPR, and can be obtained from a similar consideration involving imaginary source F' (mirror image of the focusing point F in the reflector in the auxiliary medium). Point F' is the center of curvature for the fictitious wavefront Σ^-, the same way as F is the center of curvature for the wavefront.

Quantities R^+ and R^- in Equation 3 are radii of curvature of the fictitious wavefronts Σ^+ and Σ^-. It is clear from Figure 1 that, for a given central ray, radii R^+ and R^- depend upon the position of the point F where the paraxial ray intersects the central ray and, thus, upon the position of the source and receiver that define the paraxial ray. Equations 4 and 5 give the radii of curvature of the fictitious wavefronts R^+ and R^- via the fundamental radii of curvature R_{cre} and R_{cee}, which are defined by the central ray only and are the same for all the source-receiver pairs in the vicinity of the central ray.

The dependence of radii R^+ and R^- on the position of the source and the receiver (or on the position of point F on the central ray) is contained in the focusing parameter σ, which has a very clear physical interpretation. In particular, $\sigma = 0$ means that $R^+ = R^- = R_{cee}$, which implies that point F coincides with the center of curvature of the normal wavefront (or of the reflector), and corresponds to a case of coinciding

source and receiver (zero-offset configuration). Cases $\sigma = 1$ and $\sigma = -1$ imply $R^- = 0$ and $R^+ = 0$, and correspond to common-source and common-receiver configurations. The case $\sigma = \infty$ leads to $R^+ = R^- = R_{cre}$, and corresponds to a situation where focusing point F coincides with O.

In the general case of a curved reflector and inhomogeneous overburden, Equation 6 for the focusing parameter σ is a small-offset approximation. However, for a plain (horizontal or dipping) reflector under a homogeneous overburden, Equation 6 is exact for all offsets.

The moveout correction defined by Equations 3–6 can be applied to arbitrary source and receiver offsets, as long as the arcs of fictitious wavefronts Σ^+ and Σ^- can be considered circular in shape. The moveout correction in Equation 3 is a sum of two hyperbolas. However, for a number of source-receiver distributions this correction is reduced to a single hyperbola. For a common source (common receiver) gather, this can be readily seen by substituting $\Delta X^+ = 0$ ($\Delta X^- = 0$) in Equation 3. For a CMP gather, the multifocusing moveout formula (Equation 3) is reduced to the "shifted hyperbola," Equation 2 under an assumption of locally plain-reflection interface ($R_{cee} = \infty$).

Implementation. Practical implementation of multifocusing requires determination of three imaging parameters (β, R_{cre}, and R_{cee}) for each t_0. In a conventional NMO stack, the single parameter (namely, the stacking velocity) is usually determined by means of interactive velocity analysis. This analysis consists of calculating a panel of correlation measure (e.g., semblance) as a function of t_0 and velocity, and picking an appropriate correlation maxima as a function of t_0. A similar procedure for multifocusing is impractical, for an interactive procedure would have to involve displaying and picking the maxima of the correlation measure as a function of four variables (t_0 and three unknown parameters).

Automatic mode is necessary. It is based on coherency measure calculation and its analysis of the multifocusing supergather. The procedure consists of data correction according to different traveltime curves using Equation 3 and finding parameters β, R_{cre}, and R_{cee}, which correspond to the coherency measure maximum. The correlation procedure described above is repeated for each central point and for each time sample producing an MF time section. Each sample on this section represents a stacked value corresponding to the optimal values of β, R_{cre}, and R_{cee}.

Note that such an optimization procedure optimally sums signals as well as spatially correlated noise. In this case, even the global maximum may be related to some kind of coherent noise rather than to desired signal. For example, strong multiple reflections may have a higher correlation measure than weaker primary events. This undesired effect can be avoided or reduced by using a priori information on search parameters and applying constraint optimization.

Multifocusing advantages. MF moveout correction as defined by Equation 3 can be applied to an arbitrary trace whose source and receiver locations are within a certain vicinity of an imaging point on the observation plane. The multifocusing moveout-time correction aligns reflection events not only within a single CMP gather but in a supergather, without any loss of a spatial resolution. Figure 4 shows the geometry of a typical supergather. Potential benefits of multifocusing stacking as compared to the CMP stack are as follows:

- Stacking a large number of traces covering many CMP gathers can increase the stacking power and increase sig-
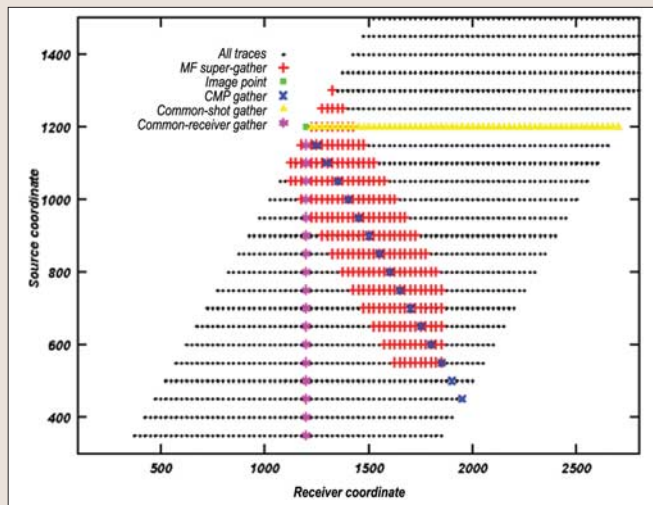

Figure 4. *Multifocusing stacking chart in shot receiver coordinates. The number of traces in the multifocusing supergather (red crosses) is many times that of a CMP, common shot, or common-receiver gather.*
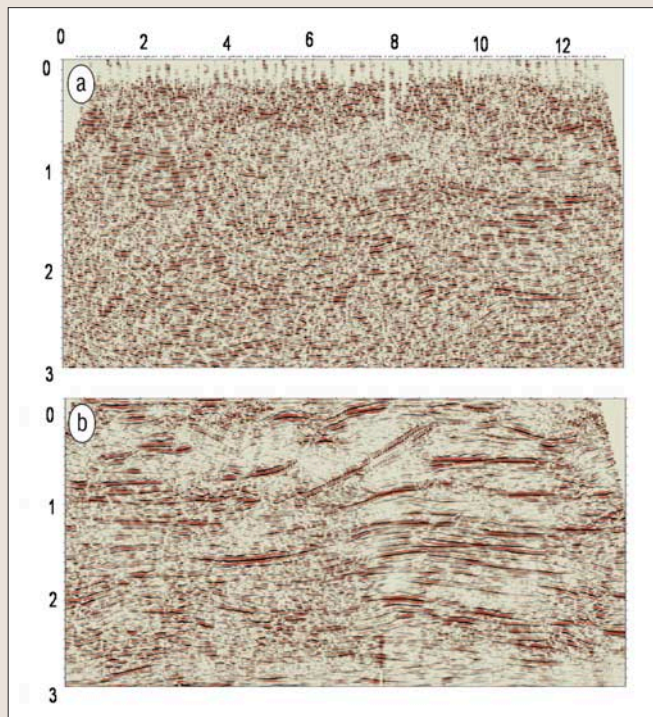

Figure 5. *CMP (a) and MF (b) stacks of six-fold data from northwestern Russia. Horizontal axis = distance (km). Vertical axis = time (s).*

nal-to-noise ratio. Typically, the number of traces in the MF supergather exceeds the CMP fold at least by an order of magnitude. This can be particularly beneficial for data with low fold and/or low signal-to-noise ratio.
- All time samples of a given reflection event on a given central trace in MF should have the same parameters within the wavelet. Thus, the moveout correction curve is parallel for all samples within the wavelet and moveout-corrected signals are stretch free.
- The MF moveout correction formula is a double square root equation that differs from the conventional NMO formula for CMP stacking. The formula describes traveltime behavior for a wider class of subsurface models.
- Definition of wavefront curvatures and emergence angle

makes it possible to determine dip-independent velocities. Hence, MF incorporates the key property of DMO processing and these velocities may be used for time migration.

- MF parameters may be estimated automatically.

Examples. The examples below represent case studies from Russia and Ukraine.

MF was applied to a low-fold old data set with 220 shot gathers and 50-m source spacing. Each shot consists of 24 traces and 50-m spacing, providing 12 fold CMP gathers. The area has complex geology, including thrust and block structures, steep dips, fractures, and a complicated shallow zone. Conventional CMP processing procedures (including deconvolution, noise reduction, DMO and poststack migration) did not provide data quality sufficient for reliable geologic interpretation (Figure 5a.)

Figure 5b shows the same data set processed by MF with the following parameters: the range of β search was between –0.7 and 0.7 radians with 0.01-radian increment; range of R_{cre} search was 70–40 000 m with 500-m increment; range of R_{cee} search was 2000 to –2000 m with 20-m increment.

The same preprocessing steps as in the conventional processing were applied to the input data for MF. One can see a substantial advantage of multifocusing over the con-
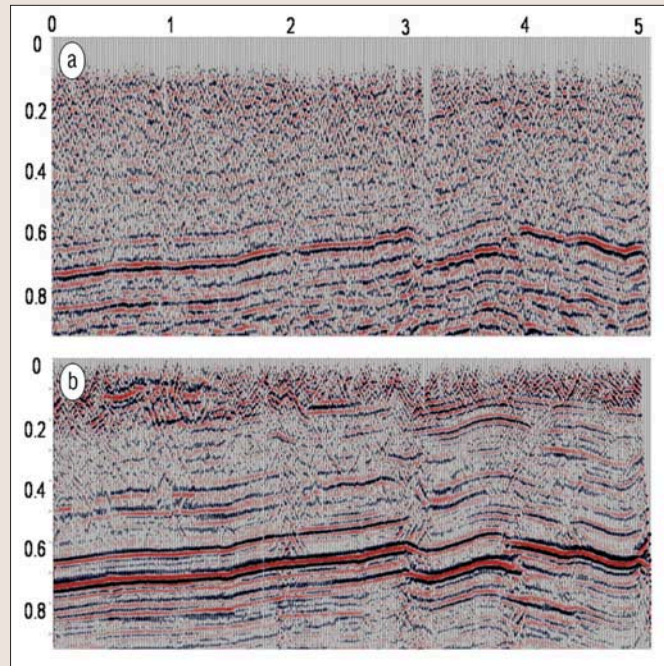

Figure 6. CMP (a) and MF (b) stacks of 24-fold data from western Siberia. Horizontal axis = distance (km). Vertical axis = time (s).
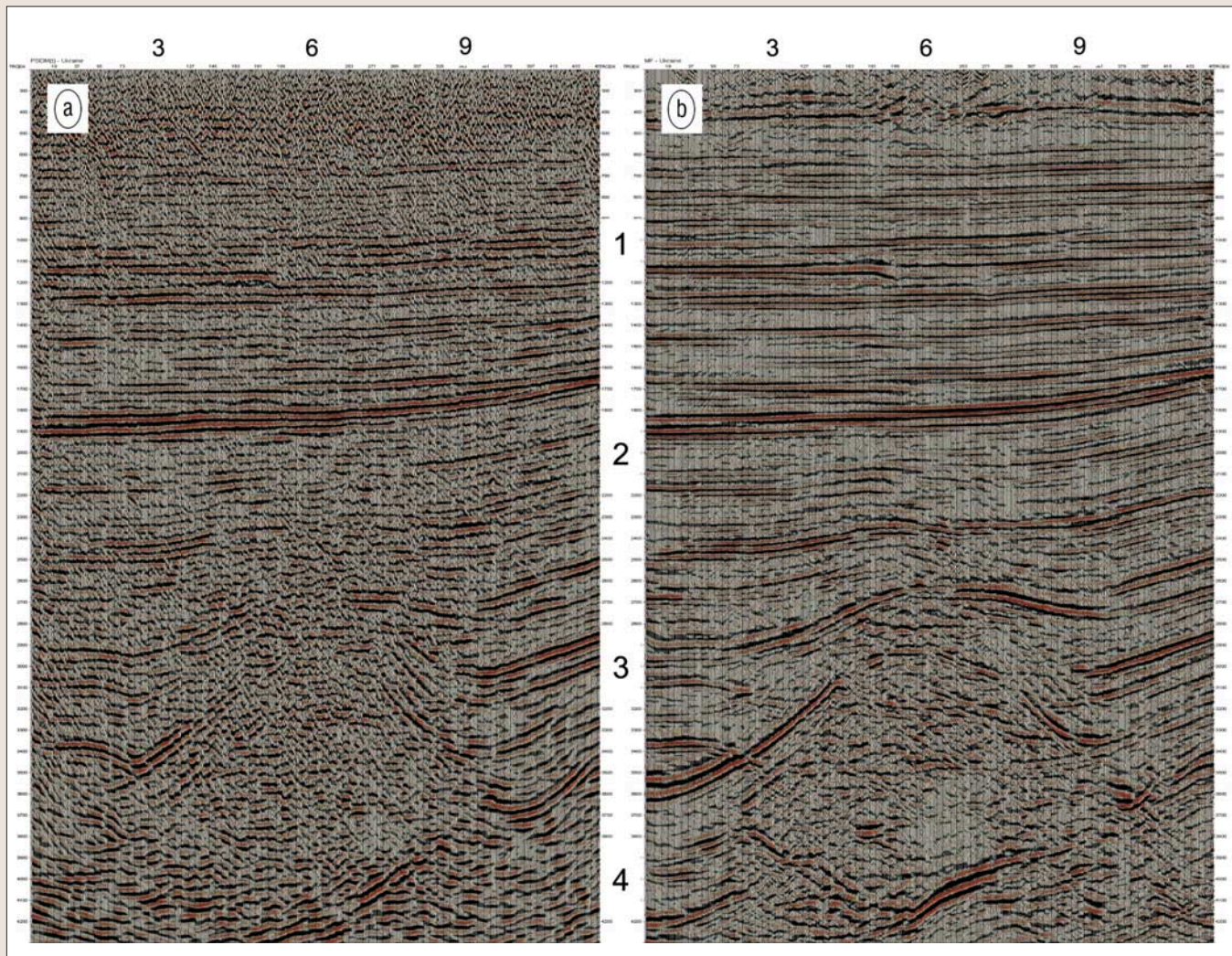

Figure 7. CMP (a) and MF (b) stacks of 12-fold data from the western Ukraine. Horizontal axis = distance (km). Vertical axis = time (s).
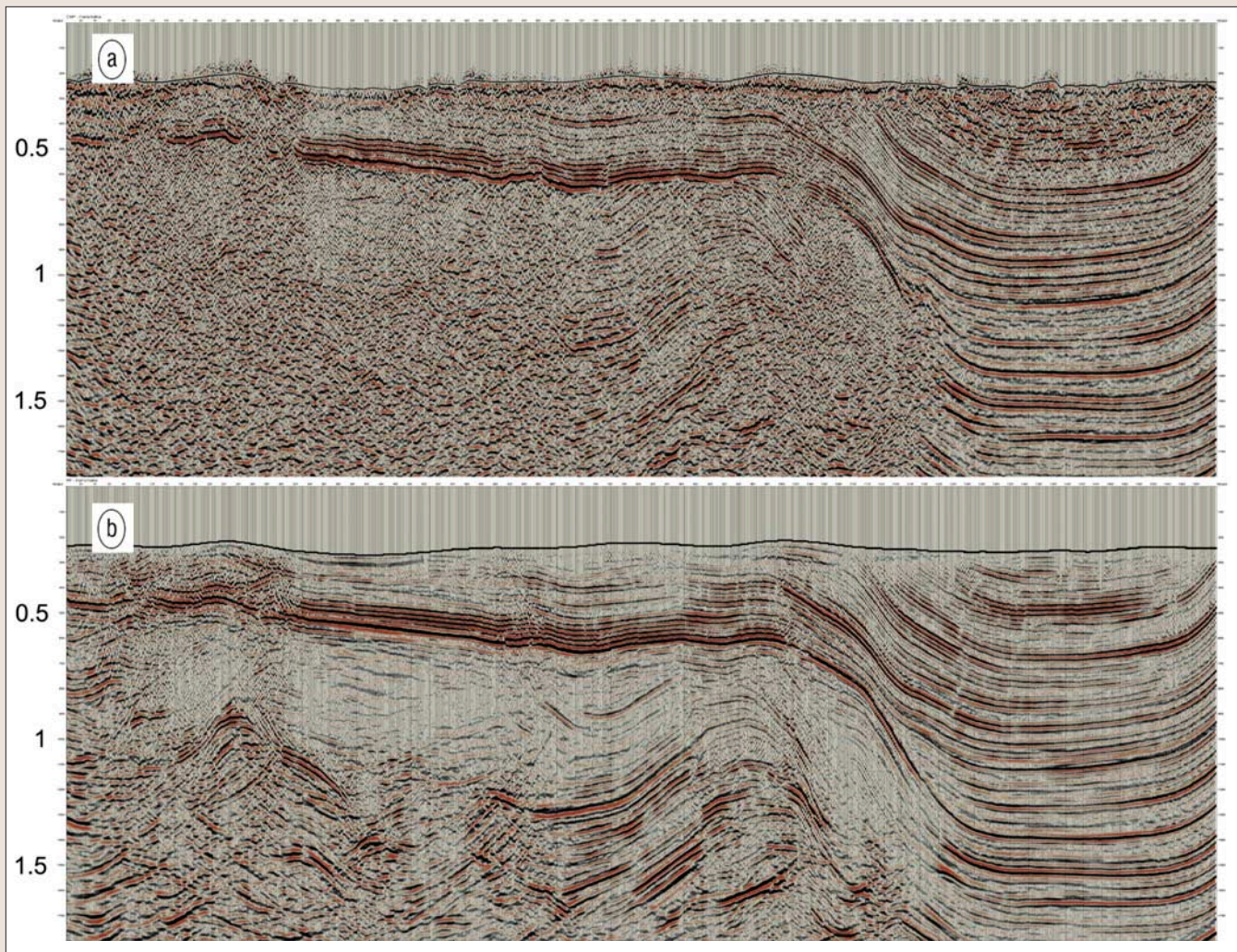
Figure 8. *CMP (a) and MF (b) stacks of 41-fold data from Kamchatka (Russia).*

ventional section. These improvements can be explained as follows. In the MF approach, ten CMP gathers are combined into a single MF supergather. Such a supergather, consisting of 120 traces, is analyzed by a parameter search procedure. Optimal triplets of the multifocusing parameters are estimated for each time sample and each CMP position. This ensures an increase of the stacking power of MF over a conventional stack by a factor of about 4.

The next example also uses an old land data set consisting of 240 shot gathers with 50-m source spacing. Each shot consists of 48 traces and 50 m spacing. The average number of traces per CMP is 24. Figure 6a shows a conventional time section after preprocessing and detailed velocity analysis. It has a low signal-to-noise ratio in the time interval 0-0.6 s and the wavefield is vague near the assumed tectonic zone.

Figure 6b shows the same data set processed by MF. Preprocessing was analogous to conventional stack. The MF parameters were: the range of β search was between –0.2 and 0.2 radians with an increment of 0.005 radian; the range of R_{cre} search was 20–50 000 m with a 100-m increment; the range of R_{cee} search was between 2000 and –2000 m with 200-m increment.

The MF section has noticeable advantages over a conventional section: increase of signal-to-noise in at shallow times and better definition of fault zones (horizontal posi-

tion of about 4 km). These improvements are caused by increasing the signal-to-noise ratio as in the previous case and absence of signal stretching in the MF moveout correction.

The following old land data set was acquired using 200 shot gathers with 100-m source spacing. Each shot consists of 48 traces and 50-m spacing. This acquisition geometry provides CMP fold of 12 traces. Figure 7a shows the results of CMP processing including Radon-based multiple suppression. Shallow reflectors (up to 1.5 s) are difficult to track, and the salt body is not well defined. Figure 7b shows the results of MF processing the following parameters: β search range between 0.3 and 0.3 radians with a 0.010-radian increment; R_{cre} search range between 70 and 20 000 m with a 100-m increment; R_{cee} search range between 2000 and –2000 m with a 100-m increment. Improvements after MF application are obvious: shallow horizons and salt body are well defined.

The next example illustrates a case with high acquisition fold when a data set consists of 1770 shot gathers with a 75-m source spacing. Each shot includes 248 traces with 50-m spacing. The average number of traces per CMP is 96. The geology of the region is characterized by complex tectonics and has block structure satiated with fractures, narrow near-fault grabens, and volcano-sedimentary deposits. Complex billowy relief and outlet of basement to the sur-

face, in addition to geological structure complexity, result in a very noisy seismic wavefield. Standard CMP processing, including detailed velocity analysis with poststack Kirchhoff migration, provided satisfactory horizon tracing only in selected areas (Figure 8a).

Figure 8b shows the same data set after MF processing with the following parameters: the β range of search was between –0.7 and 0.7 radians with a 0.01-radian increment; R_{cre} search range between 70 and 40 000 m with a 200-m increment; and R_{cee} search range between 2000 and –2000 m with an increment of 100 m.

The same preprocessing and poststack migration procedures were applied to the data. Substantial improvements over the conventional section in the left of the section are obvious. These improvements are not only because of the statistical effect of summation in supergathers but mainly due to optimization of parameter R_{cee} which is connected to reflector's curvature.

Conclusions. We illustrate application of the MF method in time imaging on real data. The method consists of stacking seismic data with arbitrary source-receiver distribution according to a new moveout correction formula. Time moveout parameters of the MF are: emergence angle of the normal ray and the wavefront curvatures for two paraxial wavefronts. The MF traveltime curve provides a better approximation of actual reflection traveltime than the standard hyperbolic one. Examples demonstrate the procedure's capability for zero-offset simulation and compare results with standard procedures. In particular, multifocusing is very effective for the processing and reprocessing low-fold CMP data, caused by MF's noise suppression wavefield parameters obtained by the multifocusing can be used for velocity model estimation, time and depth migrations.

Suggested reading. "Basic formula for multifocusing stack" by Berkovitch et al. (*EAEG 2004 Extended Abstracts*). "Multifocusing in practice" by Berkovitch et al. (*SEG 1998 Expanded Abstracts*). Homeomorphical imaging method of analyzing the structure of a medium by Gelchinsky (U.S. Patent 5103429). "Preserving far-offset seismic data using nonhyperbolic moveout correction" by Gidlow and Fatti (*SEG 1990 Expanded Abstracts*). "Normal moveout correction revisited: inhomogeneous media and curved interfaces" by de Bazelaire (GEOPHYSICS 1988). "Application of multifocusing method for subsurface imaging" by Landa et al. (*Applied Geophysics*, 1999). "A new representation of the traveltime curve of reflected waves in horizontally layered media" by Malovichko (*Applied Geophysics*, 1978, in Russian). "Higher-order moveout spectra" by May and Straley (GEOPHYSICS, 1979). "AVO and nonhyperbolic moveout: a practical example" by Ross (*First Break*, 1997). "Eigenwave based multiparameter traveltime expansions" by Tygel et al. (*SEG 1997 Expanded Abstracts*). T|E

Corresponding author: igor@geomage.com